

# **LABORATORY AND IMAGING SPECTROSCOPY OF TOURMALINE – A TOOL FOR MINERAL EXPLORATION.**

**P.N. Bierwirth**

Defence Imagery and Geospatial Organisation  
Russell Offices, Canberra  
(02) 61277291 Fax: 61277396  
Philip.Bierwirth@defence.gov.au

## **Abstract**

Tourmaline is often overlooked as an indicator for exploration and there is generally a lack of information about tourmaline NIR-SWIR spectral features. The study was initiated after it was recognised that spectral features of a tourmaline sample, collected in the field by the author, varied from any known tourmaline reference spectra. Laboratory spectral analysis of museum specimens for tourmaline end-members showed that the visible to short-wave infrared spectroscopy is complex. Species in the dravite-schorl-elbaite composition field have diagnostic spectral characteristics, both in terms of the wavelength position and strength of absorption features. Tourmaline is characterized by a series of strong absorptions in the 2100 nm to 2500 nm range. The positions of these features vary with the ionic composition of the Y-site, i.e. Mg and Al content. The feature at 2360 nm is the most diagnostic for detecting tourmaline compositions by hyperspectral remote sensing due to the magnitude of wavelength variation. Dravite has a wide diagnostic feature at 2033 nm in a part of the spectrum normally devoid of features. The positions of absorptions near 1400, 1430, 1860 and 1930 nm are also indicative of tourmaline species. MnOH related absorption features are interpreted near 2390, 2173, 1470, 1316 and 1248 nm with a Mn<sup>3+</sup> feature at 526 nm. MgOH features appear at 2320, 1822, 1365 and 1306 nm. AlOH features are interpreted at 2040 and 2200 nm while Fe features appear at 720 and 1100 nm. The field sample is identified as a relatively pure schorl based on band positions at 2204 nm, 2244 nm and 2366 nm. Image analysis of variation in the dravite-schorl composition field can be used to determine proximity to ore-bodies. This hyperspectral mapping technique, combined with the spectral information derived in this study, represents a new exploration technique for gold and base-metal deposits.

## **Introduction**

Tourmaline is essentially a group name for minerals that are the main host for the element boron in the Earth's crust. Tourmaline species minerals are found in a wide range of geological environments and are associated with the introduction of boron-rich fluids. Although tourmaline occurs in many types of hydrothermal and submarine massive-sulphide ore deposits, the role of tourmaline has rarely been examined in studies of mineral deposits (Slack,

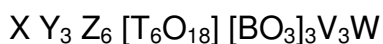
1996). Often overlooked in terms of alteration mineralogy, tourmaline presence and composition is often an indicator of economic mineralization. Tourmaline occurs in many types of world-class hydrothermal ore deposits including copper and gold deposits as well as massive sulphide base metal systems (Slack, 1996). The zone of tourmalization can closely relate to economic mineralisation or encompass the whole alteration system. Compositional variations of this mineral group are also significant for exploration. For example, tourmalines directly associated with mineralisation at Broken Hill show Mg-rich compositions relative to sulphide-free assemblages in the same area (Slack et al, 1993). Tourmaline is a valuable mineral as a proximal and distal indicator of mineralization. It is also a highly resistant mineral and remains unchanged in highly weathered surfaces including laterites. This means that studying tourmaline mineralogy is potentially a very useful exploration strategy, particularly in Australia, which has large areas of regolith-dominated terrain (Slack, 1996).

Tourmaline has unique optical and infrared (IR) spectral characteristics (Hunt et al, 1973; Clarke et al, 1990) that makes it possible for the mapping of regional mineral concentrations using hyperspectral remote sensing (Bierwirth, et al, 2002). As discussed later, at present there is little information in the literature about the influence of tourmaline composition on SWIR spectral features. This paper presents a condensed version of a PhD study of tourmaline spectral properties in relation to airborne hyperspectral observations (Bierwirth, 2004). The aim of the study was to characterize tourmaline species in terms of the spectral range useful to remote sensing and field spectroscopy, i.e. the visible to SWIR range.

### Chemistry of tourmaline

The chemistry of tourmaline is complex and the nomenclature in the early literature was confusing (Dietrich, 1985) where many of the tourmaline names that had been proposed are based on visible colour alone. More recently a naming convention has been established (Hawthorne and Henry, 1999) and there are currently 14 tourmaline end-members that have been accepted by the International Mineralogical Association (IMA).

The formula for tourmaline is expressed as:



where:

X = Na, Ca, K, □ (vacancy)

Y = Li, Mg, Fe<sup>2+</sup>, Mn<sup>2+</sup>, Al, Cr<sup>3+</sup>, V<sup>3+</sup>, Fe<sup>3+</sup>, (Ti<sup>4+</sup>)

Z = Mg, Al, Fe<sup>3+</sup>, V<sup>3+</sup>, Cr<sup>3+</sup>

T = Si, Al, B

B = B, □

V = OH, O, (F)

W = OH, F, O

The species in parentheses are not yet proven to occur at these sites. Some common tourmaline species are listed in Table 1 as a function of cation and

anion site occupancy. Liddicoatite and uvite are calcic tourmalines while the rest are classified as alkali. Many other rare species are not included in Table 1 but can be found in Hawthorne and Henry (1999). These are tourmaline end-members and this classification could still be considered to be contentious (for example Mn is not listed as a species factor in Table 1). However, it is used here to name the minerals used in this study.

Table 1. Element chemistry for cation sites X, Y Z and T and anion sites V and W in common tourmaline species (from Hawthorne and Henry, 1999)

Tourmaline Species	X	Y	Z	T	V	W
Dravite	Na	Mg <sub>3</sub>	Al <sub>6</sub>	Si <sub>6</sub>	(OH) <sub>3</sub>	OH
Schorl	Na	Fe(2+) <sub>3</sub>	Al <sub>6</sub>	Si <sub>6</sub>	(OH) <sub>3</sub>	OH
Elbaite	Na	(Al,Li) <sub>3</sub>	Al <sub>6</sub>	Si <sub>6</sub>	(OH) <sub>3</sub>	OH
Liddicoatite	Ca	(Li,Al) <sub>3</sub>	Al <sub>6</sub>	Si <sub>6</sub>	(OH) <sub>3</sub>	F
Buergerite	Na	Fe(3+) <sub>3</sub>	Al <sub>6</sub>	Si <sub>6</sub>	(O) <sub>3</sub>	F
Uvite	Ca	Mg <sub>3</sub>	Al <sub>5</sub> Mg	Si <sub>6</sub>	(OH) <sub>3</sub>	F

## Study Samples

Twelve samples were chosen from a large number of tourmalines housed in the museum in the Department of Earth and Marine Science at the Australian National University. These samples were selected to give a range of colours from specimens that had been previously verified (as part of the museum collection) as tourmalines by X-ray diffraction analysis. All samples are within the dravite-schorl-elbaite composition field. These are the most common species and are therefore likely to be of greatest relevance to remote sensing and spectroscopic studies.

Representative slices of the tourmaline crystals were analyzed with a scanning electron microscope at the Australian National University. Four measurements, from widely dispersed locations in each sample, were collected and the average of these are presented in Bierwirth (2004). A solid solution series exists between elbaite and schorl, dravite and schorl, but not between elbaite and dravite (Deer et al, 1992). Two of the analysed brown dravite samples were characterized by their high Mg content and low Fe content (Bierwirth, 2004) and relatively close to the ideal dravite composition. The three black schorl specimens have Fe ranging from 1.45 to 1.76 ions. This is high compared with other samples but low compared with 3 ions for pure schorl indicating their impurity. Also the Mg content of the schorl samples is much higher than the schorl end-member that has negligible Mg. The elbaite have typical high Al contents due to Al occupying Y sites but the Mn and Fe contents are much higher than the pure end-member (Dietrich, 1985; Hawthorne and Henry, 1999).

## Visible to short-wave infrared spectroscopy

The solar reflectance spectrum that is useful for airborne and satellite hyperspectral systems, is the range 400 to 2500 nm. For this range, there are few tourmaline reflectance spectra presented in the literature and many of these

are not specific about tourmaline species, e.g. Hunt et al (1973) and Clarke et al (1990). A number of studies review visible and near infrared spectra of tourmalines (Faye et al, 1974; Manning, 1969; Taran et al, 1993). The most commonly observed bands are the absorption features near 750nm and 1100 nm, due to energy transitions in ferric and ferrous iron respectively. Other well-defined features around 1400nm and a group of bands between 2200 and 2400 nm, some of which are thought to be due to B-O stretching modes (Hunt et al, 1973). Spectral features in the visible and near infrared (VNIR) are due to transitions between energy levels in atomic ions and charge transfer (CT) where electrons migrate between ions and ligands (Hunt, 1977). Although there are exceptions, some generalizations can be made about visible colour and composition. For example, black tourmalines are often Fe-rich, brown are Mg-rich, green are either Cr or Mn + Fe-rich, blue are Mn + Fe-rich and pink tourmalines are generally Mn-rich. These colours and element associations generally match the composition data for the samples in this study (Bierwirth, 2004).

Tourmalines currently recorded in the USGS spectral library (Clarke et al, 1990) are elbaite, the Al-rich end-member and a brown tourmaline, probably schorl or dravite although no element composition analysis is provided. Given that there exists a much larger group of tourmaline species, the spectral information currently available for this mineral group is clearly limited. This study has sought to expand on the knowledge base by providing information on a wide range of well-identified tourmaline end-members. This should be of benefit to both remote sensing studies and tourmaline species identification by using ground or laboratory-based spectrometers.

### **Visible to short-wave infrared spectroscopy results**

Laboratory spectroscopy was performed on the twelve samples using an Analytical Spectral Devices (ASD) spectrometer in the spectral range 350 to 2500 nm ( $28570$  to  $4000\text{ cm}^{-1}$ ). The illumination source was a Makita MC900 9.6V lamp and spectra were measured relative to a spectralon standard to derive reflectance. Full spectrum results showed that the three compositional groups have distinctly different spectral characteristics (Bierwirth, 2004). Schorl shows the strong absorption due to ferrous iron increasing to shorter wavelengths from 2100 nm and generally lacks features in this region. Dravites and elbaite have other well-defined absorption features around 1400 nm and between 1800 and 2100 nm. The samples T\_br and 24198 are close to the ideal composition for dravite, also indicated by their brown colour, and examples of dravite spectra are not previously represented in the literature. Characteristic spectra for the three groups are presented below.

### **The 2100 to 2500 nm spectral range**

Figure 1 shows the 2100 to 2500 nm spectral range for representative spectra of each of the three groups. There are four major spectral absorption features in this region for all samples and the elbaite exclusively have a fifth feature at 2173 nm. The four main features are near 2200, 2245, 2300 and 2360 nm but their exact positions vary considerably amongst samples. Spectral features at these wavelengths are commonly due to X-O-H stretching vibrations (Hunt,

1977) and features due to Al-OH, Mg-OH and Fe-OH are often described (Hunt et al, 1973; Clarke et al, 1990). Some previous workers (e.g. Hunt et al, 1973) believe at least some of the bands seen in Figure 1 must also be due to combinations involving the B-O stretching modes and Clarke et al (1990) suggest that all four main bands are due to B-OH.

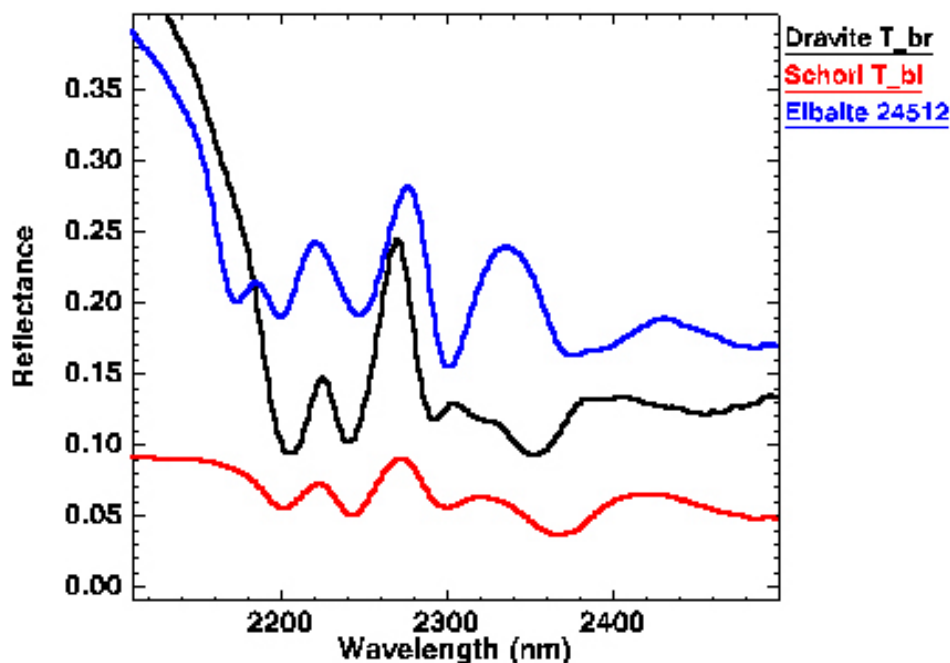


Figure 1. SWIR reflectance spectra for specimens representative of tourmaline species dravite, schorl and elbaite.

For each sample, the wavelength position for each absorption minimum was manually read from the reflectance spectra and these values were used to look for correlations with element concentrations. The variations in wavelength position for the 2200, 2245 and 2350 nm features appear to be related to Mg-content (Figures 2a to 2c), although an influence of other Y-site cations such as Fe, Mn and Al are likely to be important. In particular Mg is negatively correlated to Al for the samples ( $r = -0.83$ ). The data for the two purer dravite (highest Mg) samples coincide in Figure 2(a) and (c). These three wavelength features vary by 7, 9 and 26 nanometres respectively and although the intermediate dravite-schorl samples overlap in Figure 2a-c, the absorption positions of these features appear to be reliable indicators of tourmaline species.

The relationship in Figure 2c is the reverse of Figures 2a and 2b in that the wavelength of the centre of the 2200 nm absorption feature increases with MgO content. This appears to indicate that the feature is a result of a different ion absorption. The position at 2200 nm is typically related to Al-OH (Clarke et al, 1990) and this is a possibility in tourmalines given that Al-OH bonds are common (Deer et al, 1992). The negative correlation that exists between the absorption wavelength (near 2200 nm) and Al-content is the same relationship as for white micas (Duke, 1994). In contrast, the 2245 nm and 2360 nm features may be due to the B-O stretching modes (Hunt et al, 1973). The 2300 nm feature (Figure 1) is shorter for dravite (2293 nm) but near 2300 nm for both

schorl and elbaite. The major feature at 2173 nm is present only for elbaites and is likely to be due to Mn-OH. Shoulders are also present at 2390 nm for elbaites due to Mn-OH and 2320 nm for dravite samples due to Mg-OH bending or stretching vibrations.

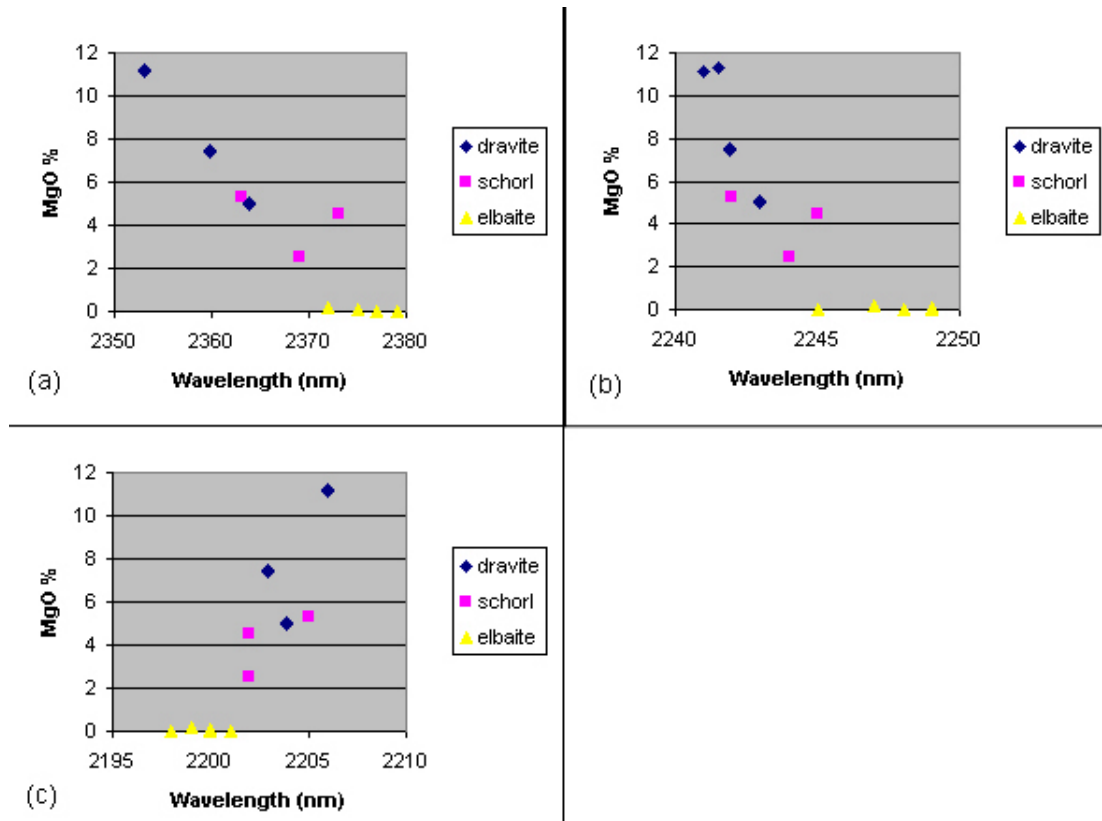


Figure 2. Wavelength position of three major SWIR absorption features (a-c) versus Mg content.

### The 1700 to 2100 nm spectral range

Spectra representing the three groups in the range 1700 to 2100 nm are shown in Figure 3. A significant and unusual feature occurs at 2033 nm for dravite, 2050 nm for elbaite (Figure 3a) and is only present as a slight shoulder near 2054 nm for schorl (Figure 3a). This part of the spectrum is normally devoid of absorption features for most minerals (Clarke et al, 1990). The features varying in position around 1850 nm and 1930 nm are probably due to H<sub>2</sub>O and the latter feature is strong for elbaites (see Figure 3a). Similar to some epidotes, these features may be due to different combinations of the OH stretching modes with lattice modes (Hunt et al, 1973). The schorl samples (Figure 3b) have weak features, possibly partly due to the suppression of ferrous iron absorption in this part of the spectrum (Clarke et al, 1990). Like the 2200 nm feature (see Figure 2c), there is a positive correlation between wavelength and Mg-content (and negative Al correlation) for both the 1850 nm and 1930 nm features. These absorption positions vary from 1922 to 1936 nm and from 1856 to 1865 nm respectively. There is also a small feature at 1822 nm for dravite probably due to MgOH.

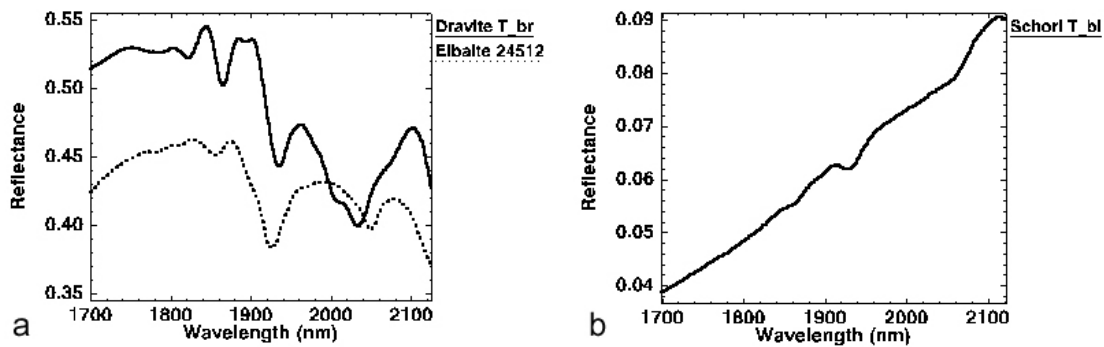


Figure 3. Reflectance of representative tourmaline species in the 1700-2100 nm spectral range.

### The 1300 to 1500 nm spectral range

Representative spectra for the range 1300 to 1500 are shown in Figure 4. Features in this region near 1400 nm are known to be due to the first overtone of the fundamental OH stretching mode, or to a combination of the fundamental stretching modes of two different OH groups (Hunt and Ashley, 1979). For multiple features to occur, there must be two or more different OH groups. Features are generally poorly defined for schorl samples (Figure 4b), again likely due to the suppression of ferrous iron absorption in this part of the spectrum (Clarke et al, 1990). The feature at 1470 nm, only present for elbaite (Figure 4a), is possibly due to MnOH and the wavelength position is apparently influenced by the Fe content (Bierwirth, 2004).

The feature near 1430, although weaker for schorl, is present for most samples. The position of this OH feature varies by only 10 nm but is apparently related to the combination of Mg and Fe (Bierwirth, 2004). Although weaker, the 1400 nm feature suggests a similar relationship between Fe+Mg content and wavelength (Bierwirth, 2004). Weaker features are also present at 1365 and 1306 nm for dravites (Figure 4a), both probably due to Mg-OH. Other weak features are present at 1316 nm and 1248 nm for the Mn-rich elbaite sample.

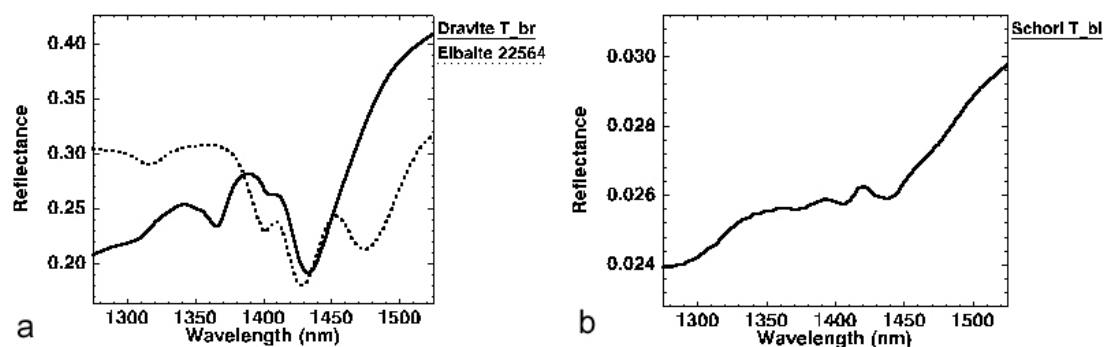


Figure 4. Reflectance of representative tourmaline species in the 1300-1500 nm spectral range.

### The VNIR spectral range

The two broad absorption bands in the VNIR range from 1080 to 1150 nm and 690 to 750 nm respectively (Bierwirth, 2004), although their broadness makes it



difficult to accurately determine the centre wavelengths. These bands are thought to be due to ferrous iron transitions (Taran et al, 1993). However the features are strong in Fe-poor dravites and suppressed for some schorls (Bierwirth, 2004) although the lowest-Fe elbaite has weaker features and small amounts of  $\text{Fe}^{2+}$  may be enough to produce the features. The  $\text{Mn}^{3+}$  feature (Taran et al, 1993) is observed at 526 nm and only for the sample with an Mn content of greater than 1.64%.

### Airborne hyperspectral sensing of tourmaline

A short example is presented here of airborne hyperspectral mapping of tourmaline. Results are extracted from an earlier work that used airborne hyperspectral data to map the distribution of both primary alteration and regolith minerals associated with different styles of gold mineralization in the Central Pilbara Tectonic Zone (CPTZ) in Western Australia (Bierwirth et al, 2002). Figure 5(a) shows the geological map for a small part of the hyperspectral survey area. Massive quartz-tourmaline veining (Aqt) intrudes Archean metasediments (Adt - Brown) and the area is covered extensively by regolith units - sandy soils (green stippled pale yellow areas) and calcrete (yellow). Figure 5(b) shows a tourmaline abundance image derived by matching the 28 SWIR bands of the airborne HyMap data to field spectral data. In this area, tourmaline is a hydrothermal mineral and zones of tourmaline alteration may be of significance as a proximity indicator for mineralization given that significant gold occurs adjacent and to the north of the largest zone (area A in Figure 5b) (Bierwirth et al, 2002). In another area in the north of the image (B), the tourmaline occurrence is previously unknown. This area is adjacent to an ultramafic unit (AaMus, Figure 5a) and the zone is mapped as surface cover (calcrete, Czrk).

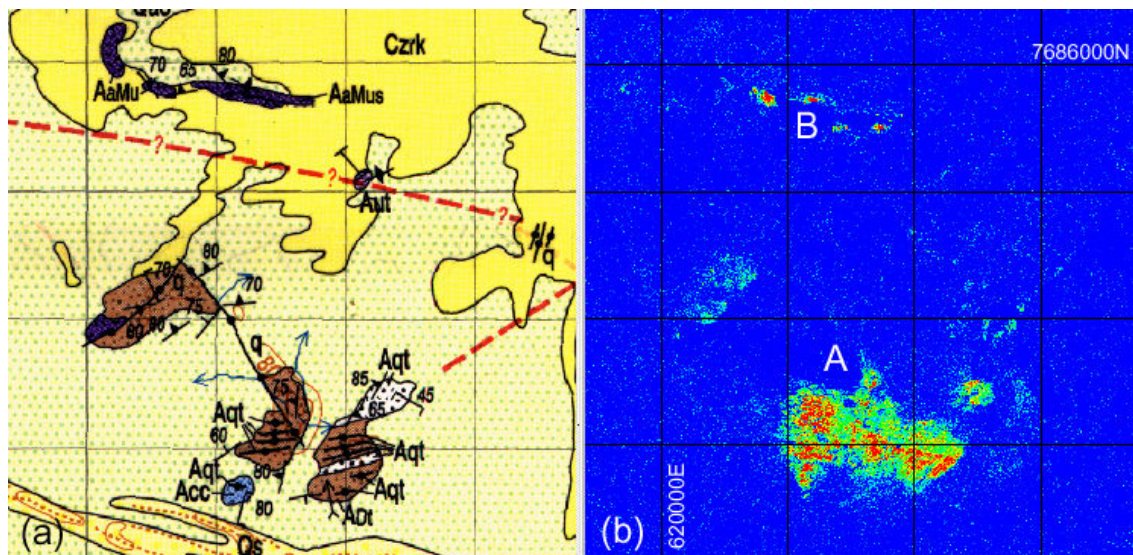


Figure 5(a) Geological map of a zone of a tourmaline occurrence (Aqt) in the Pilbara region, W.A. (from Smithies, 1999) (b) an airborne HyMap tourmaline abundance image for the same area (red is high). Grid lines are 1 km spaced in AMG coordinates.

Two fields samples of the tourmaline zone (at A in Figure 5) were analysed using the Portable Infrared Mineral Analyser (PIMA). The identification of major



tourmaline here was independently confirmed by X-ray diffraction (XRD) analysis. Based on the laboratory study, the band positions for the field spectra at 2204 nm, 2244 nm and 2366 nm identify this tourmaline as schorl (see Figure 2a-c). Given the lower spectral precision of the airborne HyMap data, probably only the 2360 nm feature could be used to approximate tourmaline composition. Given the significance to exploration, of the relative components of Mg and Fe end-members, it was decided to attempt to use the airborne data to investigate whether there were any regional spectral variations in tourmaline composition.

The approach taken here was to further analyse those pixels where tourmaline abundance had been identified, as discussed in the previous section, using the SWIR bands from 1986 nm to 2449 nm. Laboratory spectral studies above indicated that the largest wavelength shift in the dravite-schorl series was the feature near 2360nm (see Figure 1). This feature is centred at 2353 nm for dravite while schorl has the position at 2369 nm. Spectral Matched Filter (MF) analysis was used on the spectral range 2287-2433 nm to generate abundance results using laboratory end-members for dravite and schorl (see Figure 1). The results from these two end-members were then ratio-ed to produce a single colour coded image and presented only for high tourmaline abundance areas (Figure 6a). In this image, red areas show more dravite-rich (high Mg) in red grading down through yellow and green to blue indicating a more schorl-rich (high Fe) composition.

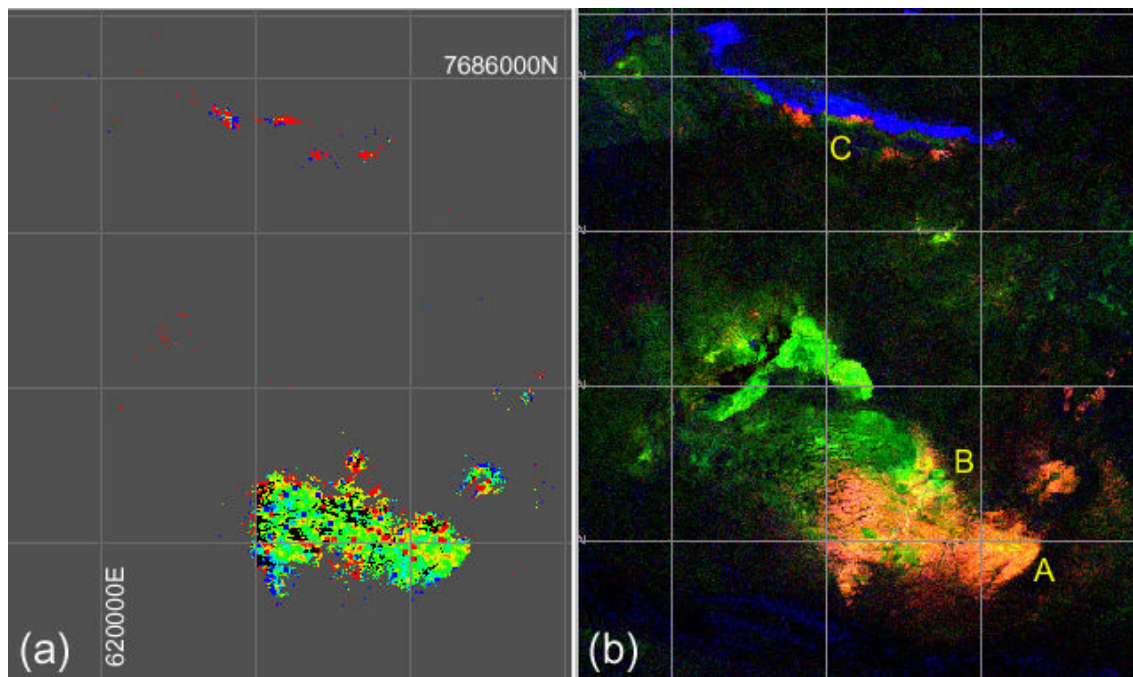


Figure 6 (a) a colour scale image indicating tourmaline composition. Red and yellow areas show more dravite-rich (high Mg) whereas green and blue areas are more schorl-rich (high Fe). (b) a colour combination of the MF abundance images for all tourmaline, white mica (low Al) and talc in red green and blue respectively. Grid cells are 1 km x 1 km in AMG coordinates.

Wavelength shifts of the 2360 nm feature were confirmed from image spectra. Some Mg-rich (dravite) tourmaline image spectra also showed features at 2040

nm and 2287 nm while Fe-rich image spectra also showed a feature at 2300 nm (Bierwirth, 2004). Comparison with the spatial distribution of other minerals in the area allows for some interpretation of the apparent variations in tourmaline composition. Figure 6b shows that Mg-rich tourmaline (red areas in Figure 6a) in the prospect area (A and B) appears to be correlated with the zones of low Al white mica (Figure 6b). This indicates that Mg-tourmaline is occurring in alteration zones along with Mg-rich (substituting for Al) white micas and these zones are primary targets for mineralisation. The tourmaline in the area to the north (C) shows a strong Mg-rich composition. As mentioned above these zones were previously unknown and again there are associations with white mica suggesting that they are exploration targets.

## Discussion and Conclusions

Clearly there is a wide range of VNIR to SWIR spectral features in tourmalines. Some of these features are common between different species while others are unique. Variations of the wavelength of features are all due to cation substitutions in the Y site of the structure. For cation substitutions involving similar valency such as  $\text{Mg}^{2+}$  to  $\text{Fe}^{2+}$ , the increase in mass can cause the band wavelength to increase (McLeod et al, 1987). Given the compositional associations with feature wavelengths, this substitution is the most likely cause of wavelength shifts for the 2245 and 2360 nm features (see Figures 1, 2a and 2b). For cations with similar mass, an increase in valency such as  $\text{Mg}^{2+}$  to  $\text{Al}^{3+}$  can lead to a shortening of wavelength of the corresponding band and this substitution could be at least part of the reason for the relationship in Figure 2c. This is conceptually similar to Tschermak substitution in white micas where a shift to longer wavelengths for the 2200 nm feature is associated with Mg-Fe-Si substitution for Al (Duke, 1994). However, the absorption features, for elbaite in Figures 2a and 2b and for schorl/dravite in Figure 2(c), cannot be explained by the same models.

Apart from the wavelength positions of the principal absorption features, a number of characteristics appear to relate exclusively to the presence of significant quantities of Mn and Mg. Mn-OH related absorption features are located at 2390, 2173, 1470, 1316 and 1248 nm while a  $\text{Mn}^{3+}$  feature occurs at 526 nm. The latter three features only appear when Mn content exceeds about 2%. Mg-OH related features appear at 2320, 1822, 1365 and 1306 nm. Al-OH related features are interpreted at 2040 and 2200 nm while Fe related features appear at 720 and 1100 nm, both of the latter influenced by only minor Fe as shown by the presence of these features in the Fe-poor dravite samples.

This study has demonstrated that data from the airborne HYMAP sensor can be processed using laboratory spectral information to quantify tourmaline abundance and to determine the species of tourmaline. The 2360 nm feature is probably the most useful for species identification due to the wide range in wavelength position of this feature in tourmalines. Although the spectral resolution of HYMAP may not be quite precise enough to identify the exact composition, image processing was able to detect Mg-rich versus Fe-rich zones in the Pilbara. This study has provided important spectral data for aiding tourmaline species identification using spectroscopy and remote sensing.

However, the chemistry of tourmaline is complex with a wider range of species than studied here and hence a larger study is recommended.

### **Acknowledgements**

The authors wish to thank John Vickers (ANU) for microprobe sample preparation, Guy Byrne and Susan Campbell (CSIRO) for their assistance with the ASD spectrometer. I would also like to thank Watcharaporn Keankeo (Burapha University, Thailand) for her assistance in calculating ionic proportions and general support.

### **References**

- Bierwirth, P.N., 2004, Methods of spectral geology utilizing airborne-hyperspectral and satellite remote-sensing applications for exploration and acid-mine drainage. *PhD Thesis*, Australian National University, 212p.
- Bierwirth, P.N., Blewett, R. S., and Huston, D. L., 2002, Hyperspectral mapping of mineral assemblages associated with gold mineralization in the West Pilbara, W.A. *Economic Geology*, 97: 4, 819-826.
- Clarke, R. N., King, T.V.V., Klejwa, M., and Swayze, G.A., 1990, High Spectral Resolution Spectroscopy of Minerals. *Journal of Geophysical Research*, 95: B8, 12,653-12,680.
- Deer, W.A., Howie, R.A., and Zussman, J., 1976, An introduction to the Rock Forming Minerals. Longman, London, 528p
- Dietrich, R.V., 1985. The tourmaline group. Van Nostrand Reinhold, New York, 300p.
- Duke, E.F., 1994, Near infrared spectra of muscovite, Tschermak substitution, and metamorphic reaction progress: implications for remote sensing: *Geology*, 22: 621-624.
- Faye, G.H., Manning, P.G., Gosselin, J.R., and Tremblay, R.J., 1974, The Optical Absorption Spectra of Tourmaline: importance of the charge-transfer process. *Canadian Mineralogist*, 12: 370-380.
- Hawthorne, F.C., and Henry, D.J., 1999, Classification of the minerals of the tourmaline group. *European Journal of Mineralogy*, 11: 201-215.
- Hunt, G.R., Salisbury, J.W., and Lenhoff, C. J., 1973, Visible and Near Infrared Spectra of Minerals and Rocks: VI. Additional Silicates. *Modern Geology*, 4: 85-106.
- Hunt, G.R., 1977, Spectral Signatures of Particulate Minerals in the Visible and Near Infrared. *Geophysics*, 42: 501-513.
- Hunt, G.R., and Ashley, R.P., 1979, Spectra of Altered Rocks in the Visible and Near-Infrared. *Economic Geology*, 74: 1613-1629.
- Manning, P. G., 1969, Optical absorption spectra of chromium-bearing tourmaline, black tourmaline and buergerite. *Canadian Mineralogist*, 10: 57-70.

McLeod, R.L., Gabell, A.R., Green, A.A. and Gardavski, V., 1987, Chlorite infrared spectral data as proximity indicators of volcanogenic massive sulphide mineralisation: in *Pacific Rim Congress*, 87: 1-4.

Slack, J. F., 1996, Tourmaline associations with hydrothermal ore deposits. In: Boron mineralogy, petrology and geochemistry. *Reviews in Mineralogy*, 33.

Slack, J.F., Palmer, M.R, Stevens, B.P.J, and Barnes, R.G., 1993, Origin and significance of tourmaline-rich rocks in the Broken Hill district. *Economic Geology*, 99: 3.

Smithies, R.H., 1999, Geology of the Yule 1:100,000 sheet: Western Australia Geological Survey, 1:100,000 series explanatory notes, Sheet 2556, 15 p.

Taran, M.N., Lebedev, A.S., and Platonov, A.N., 1993, Optical absorption spectroscopy of Synthetic Tourmalines. *Physics and Chemistry of Minerals*, vol 20: 209-220.